

Simulated Response of Electrochemical Sensors for Monitoring Molten-Salt Fueled Reactors

Devin Rappleye, Milan Stika, and Michael F. Simpson

Department of Metallurgical Engineering, University of Utah, 135 S 1460 E Rm 412, Salt Lake City, UT 84112 Email: d.rappleye@utah.edu

Advanced reactor concepts featuring molten salts as either the primary coolant or the actual fuel are gaining increased interest from DOE and the nuclear power industry. Examples include the Advanced High Temperature Reactor from Oak Ridge National Laboratory, the Waste Annihilation Molten Salt Reactor from MIT, and the Accelerator Driven Sub-Critical Molten Salt reactor from Texas A&M. These advanced nuclear reactor concepts are anticipated to be deployed in the future within and outside the US, potentially including non-nuclear weapon states. Traditional international safeguards approaches rely heavily upon material accountancy, but that may be insufficient for these systems due to the quantities or concentrations of TRU elements in the fuel salt. Continuous and unattended process monitoring should be an effective supplemental safeguards measure in this case to complement material accountancy. This approach, however, requires robust sensors that are sufficiently sensitive to actinide concentrations in the fuel salt. Voltammetric methods which utilize a simple three-electrode probe have widely been studied for this application—including cyclic, square wave, and normal pulse voltammetry. Based on the measured electrode potentials and peak heights, these methods can generally be correlated to concentrations of actinides and other ions in the salts. Some limitations to these methods may stem from the multi-component nature of these fuel salts. Most voltammetry studies published have focused on single actinides in a matrix salt. Even in single component studies, quantitative signal responses were found to be limited to a low range of concentrations. To provide the fundamental basis for development of advanced voltammetry systems that avoid or minimize these issues, a model called Enhanced REFIN with Anodic Dissolution (ERAD) was used to calculate voltage responses in molten LiCl-KCl with a range of UCl₃ and ThCl₄ concentrations. The model was developed based on first principles of mass transfer and electrochemistry. Based on ERAD simulations, the voltage response due to variations in hydrodynamic conditions and geometric configurations differs depending on the species present. Understanding the effect of these variations on voltage response is critical to developing electrochemical sensors and techniques for monitoring molten salt concentrations in advanced reactors.

Introduction

The Molten Salt Reactor (MSR) is a non-classical reactor concept originally developed in 1960s by Oak Ridge National Laboratory (ORNL). It has enjoyed renewed interest at the beginning of 21st century with the creation of Generation IV Reactors International Forum (GenIV). This reactor employs several distinct features—it is a high-temperature liquid-fuel system with breeding capability in thorium-uranium fuel cycle. The liquid nature of the fuel permits the employment of on-line refueling and recycling. These features bring advantage in economy and safety terms, as well as a substantial reduction of hazardous waste.

Due to the liquid state of the fuel, nuclear material is continuously being transferred between the reactor and supporting process equipment. Most importantly, on-line recycling extracts newly bred

This is accepted pre-print of the article published in Journal of Nuclear Materials Management.

Citation details: Rappleye, D., Stika, M., & Simpson, M. F. (2014). Simulated Response of Electrochemical Sensors for Monitoring Molten-Salt Fueled Reactors. Journal of the Institute of Nuclear Materials Management, 43(1), 50–56.

U-233 (or its precursor Pa-233). The amount of U-233 and thorium (Th) flowing into and out of the reactor needs to be accurately monitored in order to keep the reactor precisely critical and meet safeguards goal.

Molten Salt Reactor Design

Various designs of MSR exist [1, 2, 3, 4]. In general, the MSR operates at high temperatures (650-850°C) and uses LiF, LiF-BeF₂ (FLiBe), LiF-NaF-KF (FLiNaK) or another fluoride salt loaded with U and/or Th. This work focuses on a thorium-fueled MSR. A thorium-fuel MSR can be a single- or two-salt system, operated in either the thermal or fast neutron spectrum. As shown in Figure 1, in a two-salt system, a thorium-rich or “blanket” salt surrounds the reactor core. The other salt is uranium-rich and forms the core of the reactor.

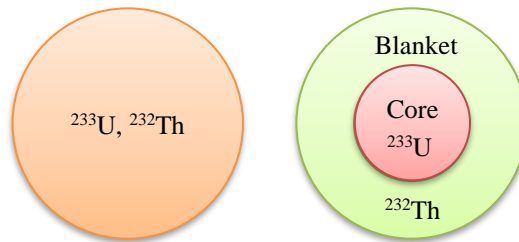
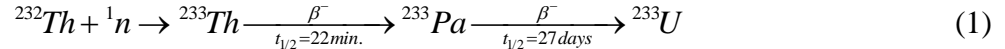


Figure 1: Depiction of a single-salt (left) and a two-salt (right) reactor

In a thorium fueled reactor, U-233 is produced when Th-232 absorbs a neutron and undergoes two beta decays, as shown below:



The first beta decay from Th to protactinium (Pa) has a half-life of 21.83 min. and can be assumed to primarily occur in the reactor. Subsequently, Pa-233 is removed from the reactor salt since it has a longer half-life of 27 days and a high neutron absorption cross section. Then, Pa-233 is allowed to decay to U-233 outside of the reactor in a hold-up tank. At this point, U-233 could be returned to the salt containing Th, if the MSR uses a one-salt system, or it could be loaded into the core salt. In either system, U will be present with Th. In a one-salt system, the weight percent of U and Th could be 1 and 40 wt%, respectively [5]. In the two-salt system, a small amount of Pa-233 will have decayed to U-233 while still in the reactor or some Th may be co-extracted with U. Thus, an ability to detect the presence and concentration of U in the presence of Th would be vital for any measurement technique.

Safeguards of MSR

Due to the continuous flow of fluids in MSRs, they would need to be treated as a bulk facility, like PUREX, rather than an item facility, like a light-water reactor. However, unlike a bulk facility, the inventory is undergoing continuous nuclear reactions which constantly change the concentration of special nuclear material within a given unit. Additionally, system clean-outs would be even more costly to a nuclear power plant, than a fuel cycle facility, because electricity cannot be stored to meet its constant demand during outages. Thus, an unattended monitoring system (UMS) that can

This is accepted pre-print of the article published in Journal of Nuclear Materials Management.

Citation details: Rappleye, D., Stika, M., & Simpson, M. F. (2014). Simulated Response of Electrochemical Sensors for Monitoring Molten-Salt Fueled Reactors. Journal of the Institute of Nuclear Materials Management, 43(1), 50–56.

accurately measure the concentration of U and Th in a salt mixture is recommended to reduce the inspection burden on the IAEA and minimize interruptions to reactor operations.

Voltammetry is an attractive option for the UMS in a MSR that could potentially provide near-real-time measurements of concentration of elements, particularly uranium and thorium, in influent and effluent streams of the reactor. It requires simple sensors that can withstand the high temperatures and the radiation environment. Several methods of voltammetry are available, such as: cyclic voltammetry (CV), linear sweep voltammetry (LSV), chronoamperometry, etc. The premise of each technique is to adjust the potential and measure the response of the current. Based on the current values, concentrations or species properties (e.g. diffusion coefficients) can be determined. One issue that can complicate voltammetric measurement is a high background current due to solution resistance. A MSR is particularly well-suited for voltammetry due to the low electrical resistivity of molten salts which have very low or negligible background currents.

Simulation of U and Th in molten salt

To investigate the feasibility and applicability of voltammetry to MSRs, the reduction peak(s) in CV or LSV of molten salt containing U and Th were simulated using a model called ERAD (Enhanced REFIN with Anodic Dissolution). ERAD has been validated by simulating the CVs of U and plutonium from open literature and comparing the results [6, 7]. Because ERAD is based on fundamental electrochemical relations, it requires several well-characterized properties for each element, including: standard reduction potentials, activity coefficients, diffusion coefficients, oxidation state, transfer coefficients and exchange current density. Unfortunately, the electrochemical data for actinides in fluoride salts (i.e. LiF, FLiBe, FLiNaK) is sparse [8]. However, significant research has been performed on eutectic LiCl-KCl salt due to the development of pyroprocessing in the U.S. under the Integral Fast Reactor (IFR) program and by other countries. Thus, the eutectic LiCl-KCl system was used for this work as an analog to a fluoride salt system. The trends and behaviors of U and Th noted in this work will be assumed to be applicable to fluoride salts. This is not an unreasonable assumption. Indeed, the limited existing electrochemical data of actinides in fluorides have been shown to be similar to their data in chlorides. Furthermore, the behavior of actinides in even less chemically similar systems, such as the aqueous and molten salt systems, has been shown to be analogous [9, 10].

As noted earlier, there exists a likely possibility that, in a MSR, small amounts of U would be found in mixtures containing significantly more Th. Therefore, the ability to make quantitative measurements of the concentration of U in a mixture containing a significant amount of Th using voltammetry is of particular interest in this work. Currently, there has been limited experimental work on application of voltammetry to LiCl-KCl eutectics containing more than one actinide in the matrix salt [11]. Therefore, this simulation work attempts to also address the analysis of voltammograms of LiCl-KCl containing multiple actinides.

Voltammetry Simulations

The properties used to simulate the electrochemical behavior of U and Th in eutectic LiCl-KCl salt at 500°C are displayed in Table 1. The standard apparent potential, diffusion coefficient, valance state, standard exchange current density and transfer coefficient are represented by E^o , D , z , i_o , and α , respectively. The number in brackets indicates the reference from which the value was taken.

This is accepted pre-print of the article published in Journal of Nuclear Materials Management.

Citation details: Rappleye, D., Stika, M., & Simpson, M. F. (2014). Simulated Response of Electrochemical Sensors for Monitoring Molten-Salt Fueled Reactors. Journal of the Institute of Nuclear Materials Management, 43(1), 50–56.

Unfortunately, ERAD is not currently capable of simulating the multiple oxidation states of an element. Therefore only +3 oxidation state was captured for U. Th is supposed to only exist in the +4 oxidation state [8, 12]. It should also be noted that interaction of U and Th metal deposits and its effect on the voltammograms is not captured in these simulations. However, previous work has shown that at 500°C no intermetallic is formed between U and Th and the solubility of U in Th is low [13, 14].

Table 1: Properties used for simulations

Property	U	Th
E° (V vs. Ag/AgCl)	-1.274 [15]	-1.325 [12]
D ($\times 10^5$ cm ² /s)	2.00 [6]	4.46 [12]
z	+3	+4
i_o (A/cm ²)	1.00 [6]	0.8*
α	0.5*	0.5*
*Assumed Value		

Table 2: Compositions of simulated runs

Calibration Data						Unknowns		
Run	U (wt%)	Th (wt%)	Run	U (wt%)	Th (wt%)	Run	U (wt%)	Th (wt%)
1	0.00	1.00	9	0.50	1.00	17	0.05	2.00
2	0.00	1.50	10	0.50	1.50	18	0.25	1.25
3	0.00	3.00	11	0.50	3.00	19	0.75	0.50
4	0.10	0.00	12	1.00	0.00			
5	0.10	1.00	13	1.00	1.00			
6	0.10	1.50	14	1.00	1.50			
7	0.10	3.00	15	1.00	3.00			
8	0.50	0.00	16	0.60	1.40			

Several simulations were performed at varying levels of U and Th concentration. The concentration values used for each run are displayed in Table 2. The first 16 simulations were used for calibrating the current-potential (i -E) curves to the weight percent values. The last 3 simulations were used as unknowns to test the performance of voltammetry in making concentration measurements. For each run, the potential was scanned from -1 to -2 V vs. Ag/AgCl(1 wt%) at a rate of 0.1 V/s, essentially a LSV, and the current was calculated based on a surface area of 4.53 cm² for the sensing (working) electrode.

The i -E curve for Run 13 is provided in Figure 2 to illustrate key features of the reduction peak that are common to all runs. Due to the proximity of U's and Th's apparent standard potentials to each other ($\Delta E^{\circ} = 51$ mV), the reduction peaks of U and Th almost completely overlap, as seen in Figure 2. This makes deciphering their separate peaks and respective peak heights impossible. Thus, the traditional method of relating peak height to concentration cannot be used. An alternative analysis method must be used.

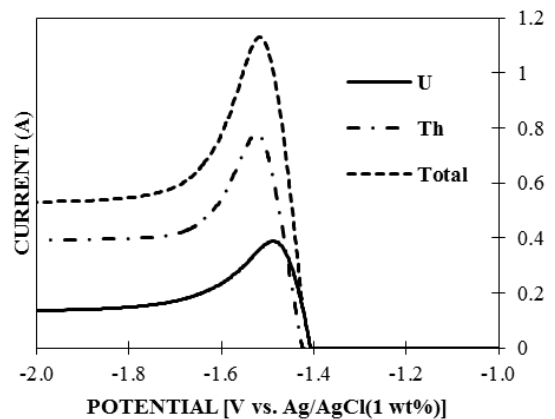


Figure 2: i -E curve for Run 13 from Table 2

This is accepted pre-print of the article published in Journal of Nuclear Materials Management.

Principal Component Regression

Principal component regression (PCR) is a multivariate analysis method which uses a greater amount of the data collected in a CV than the univariate analysis of peak height. PCR analyzes a set of data (training set) to determine the main contributors, principal components (PCs), to variance in the training set. Then using least-squares regression, a select number of the PCs are used to predict related variables from unknown data. The advantage of using PCs is that it retains the most useful information from the data while discarding the noise. However, just like any other analysis method, in order to make predictions using PCR, the conditions under which the unknown data is collected need to be the same as conditions of the training set. Only a brief explanation of PCR will be provided here, more in-depth descriptions can be found elsewhere [16, 17, 18].

The general approach to PCR is to compile a matrix ($n \times m$), called A , containing a training set of data. In this case, the training set would be the LSVs generated for Runs 1-15 (i.e. $m = 15$ samples) in Table 2. The voltammograms in the training set need to be of the same length (n data points) and scale. Then, the PCs of the training set are found by using singular value decomposition (SVD) such that:

$$A = USV^T \quad (2)$$

where U is a $n \times n$ matrix containing the PCs or the eigenvectors of AA^T , S is a $n \times m$ diagonal matrix containing the eigenvalues, V is a $m \times m$ matrix containing the eigenvectors of $A^T A$. The main thing to note is that the PCs are contained in U and are essentially vectors in an abstract coordinate system which describe the variance of the training set.

Once the PCs are determined, the number of PCs to be retained needs to be determined. The method used for selecting the number of PCs to retain will be discussed later. For now, k will represent the number of PCs retained. It should be noted that k cannot exceed the number of observations (m). Having selected k , A is projected onto the selected PCs.

$$A_{proj} = U_k^T A \quad (3)$$

U_k is a $n \times k$ matrix containing columns 1 through k of U . Next, a matrix (B), containing the regression coefficients relating concentration to the selected PCs is formed.

$$B = CA_{proj}^T \left[A_{proj} A_{proj}^T \right]^{-1} \quad (4)$$

C is a $l \times m$ matrix with the concentration values of l components in the sample. In this case, $l = 2$ for U and Th. The concentration of an unknown data set (X) can now be calculated by projecting it onto the PCs and multiplying by B .

$$C_{unk} = B \left[U_k^T X \right] \quad (5)$$

In this work, the value for k was determined using the PRESS (Predicted Residual Error Sum of Squares) method. When selecting a value for k , it is important to reduce the error in the predicted variables and include all important features of the LSV while excluding noise and not over fitting

This is accepted pre-print of the article published in Journal of Nuclear Materials Management.

Citation details: Rappleye, D., Stika, M., & Simpson, M. F. (2014). Simulated Response of Electrochemical Sensors for Monitoring Molten-Salt Fueled Reactors. Journal of the Institute of Nuclear Materials Management, 43(1), 50–56.

the data. Run 16 was used to select a value for k . The concentration of Run 16 was predicted using (5) and the residual sum of the squares (RSS) was computed by the following:

$$RSS = \sum_{l=1}^2 (C_l - C_{unk,l})^2 \quad (6)$$

where C_l represents the actual concentration of the l -th component. This calculation was repeated for $k = 1$ to 15 and the RSS of U and Th concentrations was plotted versus k for Run 16. As seen in Figure 3, the error is greatly reduced after the first 2 PCs making 3 a tempting choice for k . However, inspection of the residuals of predicted and actual i-E curves in Figure 4 show that for $k = 3$ features of the LSV are not accurately captured, such as the tail of reduction peak. At $k = 6$, all of the features of the LSV are captured. Thus, 6 PCs were used to predict the concentrations of Runs 17-19.

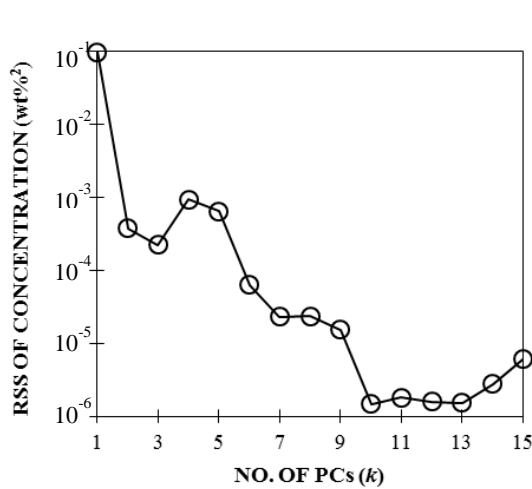


Figure 3: Semi-log plot of RSS of concentration

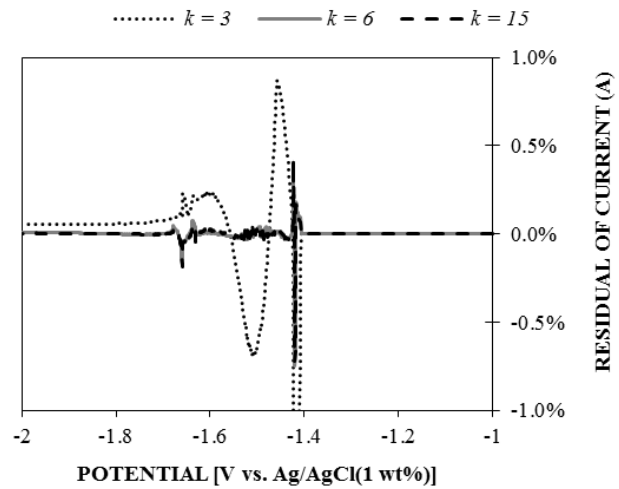


Figure 4: Residuals of the predicted current for Run 16

Results

Using PCR with 6 PCs, as described earlier, the concentrations of U and Th were predicted for Runs 17-19. As shown in Table 3, the predicted weight percent of U and Th are very close to the actual for each run with the exception of U in Run 17. Excluding the error of U in Run 17, the average error was 1.1% with a maximum of 2.8%.

Table 3: Predicted weight percent of U and Th

Run	U (wt%)		Th (wt%)	
	Predicted	Actual	Predicted	Actual
17	0.025	0.050	2.012	2.000
18	0.257	0.250	1.248	1.250
19	0.757	0.750	0.494	0.500

In order to examine the sensitivity of PCR to perturbations in the sampling environment, Run 18 was re-simulated with a change of $\pm 2.5\%$ and 5% in the diffusion layer thickness (δ) and surface

area of the sensing electrode (A). These are two parameters that could vary during the operating lifetime of an electrochemical sensor. Depending on the placement, the sensor could be in flowing or stagnant salt. If placed in flowing salt, the flow could vary during the operation of the MSR. The sensing electrode could corrode over time or become partially covered with crud altering the active surface area. Thus, understanding the effects of perturbations in δ and A on LSVs and predictions made using PCR would be helpful for determining whether an unknown LSV can be properly analyzed using an existing training set. If the conditions become too far perturbed, a new training set could be generated but this would require extensive sampling of the salt in the MSR.

Plots of the LSVs at varying A -values and δ -values can be found in Figures 5 and 6. As shown in Figure 5, the change in area affects the overall height and width of the reduction peak. On the other hand, as seen in Figure 6, δ only affects the tail of the reduction peak by causing the current to decrease with increasing δ . This is as expected since the hydrodynamic conditions should only affect the diffusion controlled portion of the reduction peak.

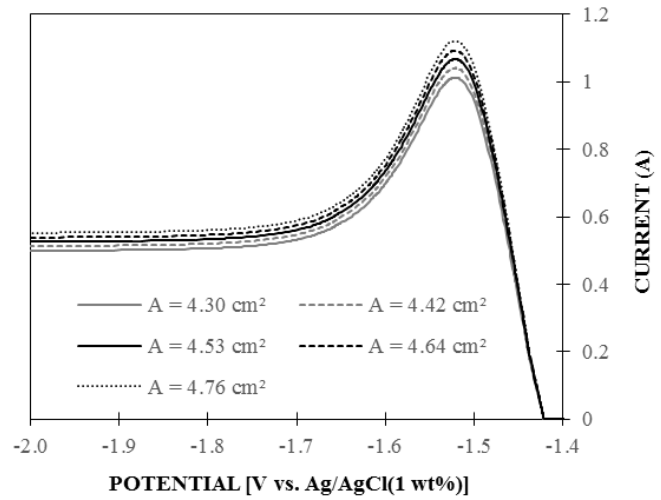


Figure 5: i -E curve for Run 18 with varying A

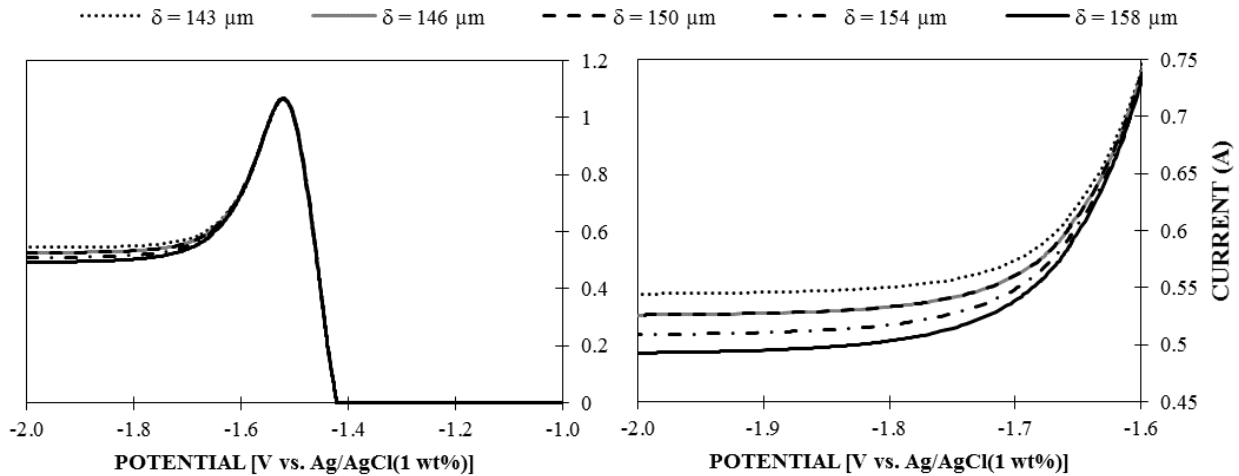


Figure 6: i -E curve for Run 18 at varying δ with magnification (right)

In order to analyze the effect of the perturbations on the predicted concentration for Run 18, PCR was applied to the curves in Figures 5 and 6 using the training set generated under the original conditions (i.e. $\delta = 150 \mu\text{m}$, $A = 4.53 \text{ cm}^2$). The predicted concentrations of U and Th are plotted in Figures 7 and 8, respectively, for the perturbed and original conditions. As can be seen in the figures, changes in the diffusion layer thickness ($\Delta\delta$) have a greater effect on the predicted weight

percent of U and Th than changes in electrode area (ΔA). In the case of ΔA , Th absorbs the majority of the error. Alternatively, U absorbs most of the error in the case of $\Delta\delta$.

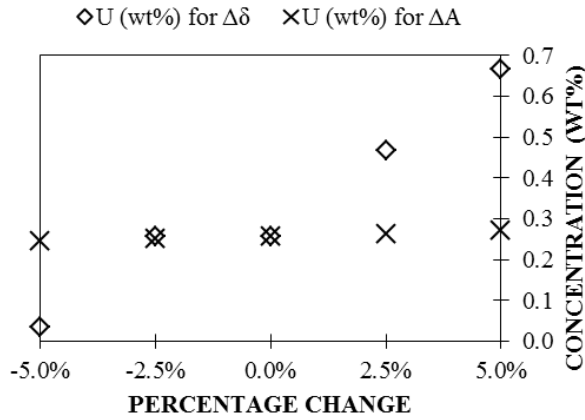


Figure 7: Effect of $\Delta\delta$ and ΔA on predicted U (wt%)

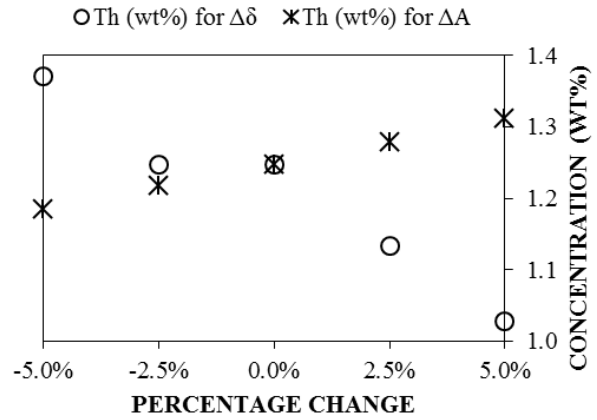


Figure 8: Effect of $\Delta\delta$ and ΔA on predicted Th (wt%)

It is quite unexpected that $\Delta\delta$ would have a greater effect on the predictions, since it had less of an effect on the LSV. However, this demonstrates that PCR, in the range tested, could be more sensitive to $\Delta\delta$, or in other words, hydrodynamic conditions, than ΔA . Thus, the placement of the electrochemical sensor in a hydrodynamically stable environment would be an important consideration when designing a UMS for a MSR. Additionally, it would be important to develop a protocol for determining the sensing electrode surface area *in situ*, as that can affect the predictions. This could be done by simply varying the length of the electrode immersed in the salt and observing the effect on the height of the reduction peak [19].

Future Work

The ability of PCR to accurately predict the concentrations of U and Th from the simulated, overlapping reduction peaks of U and Th is promising, but practical application of voltammetry to MSRs has several challenges. First, the detection of trace amounts U with Th present needs to be addressed, as the prediction of U in Run 17 had an error of 50% (see Table 3). Anodic stripping voltammetry may be more suitable for detecting trace amounts of U. Greater accuracy may be achieved in actual fluoride salts because, the apparent standard potentials (E_o') of U and Th in fluorides could have greater separation. For example, at 773 K, according to thermodynamic calculations, the difference in the standard apparent potentials of U and Th ($\Delta E_o'$) is 366 mV in FLiBe and preliminary measurements show that $\Delta E_o' = 320$ mV in FLiNaK [9, 20]. In this work, $\Delta E_o' = 51$ mV (see Table 1). However, this could come at a cost, the greater separation is created by E_o' of Th becoming even more negative than the E_o' of U, possibly causing the Th reduction peak to overlap with alkali metal reduction. A CV of Th in FLiNaK shows only a shoulder due to the commencement of reduction of one of the alkali metals in the matrix salt [20]. Another issue is that voltammetry is best suited for dilute concentrations (i.e. <10 wt%). As mentioned earlier, Th concentration could be as high as 40 wt%. This could be resolved by diluting the sample with a known amount of matrix salt (e.g. FLiBe). Although, this would make the ability to accurately detect trace amounts of U even more important.

This is accepted pre-print of the article published in Journal of Nuclear Materials Management.

Conclusions

Voltammetry is a candidate method for the online monitoring of the concentrations of U and Th in a MSR. However, LSV simulations of the U and Th reduction peaks in LiCl-KCl showed that the peaks can potentially overlap completely. Thus, traditional peak height analysis could not be used to predict the concentrations. PCR was used to predict the concentrations of U and Th. It was found that PCR provided accurate predictions except at low U concentrations. The prediction of U and Th concentrations in fluoride may be easier due to a greater separation of their standard potentials. However, there may still be complications due to interference from the matrix salt. In either case, PCR provides a powerful tool that can be used to better capture the variance of the voltammetry signals with changes in the concentrations of U and Th.

Acknowledgements

Special thanks to Riley Cumberland and Man-Sung Yim for providing and supporting the authors' use of ERAD.

References

- [1] Transatomic Power, "Technical White Paper v 1.0.1," March 2014. [Online]. Available: http://transatomicpower.com/white_papers/TAP_White_Paper.pdf. [Accessed 14 April 2014].
- [2] V. Ignatiev, O. Feynberg, I. Gnidoi, A. Merzlyakov, V. Smirnov, A. Surenkov, I. Tretiakov and R. Zakirov, "Progress in Development of Li,Be,Na/F Molten Salt Actinide Recycler & Transmuter Concept," in *Proceedings of ICAPP*, Nice, 2007.
- [3] E. Merle-Lucotte, D. Heuer, M. Allibert, V. Ghetta, C. Le Brun, R. Brissot, E. Liatard and L. Mathieu, "The thorium molten salt reactor: Launching the thorium cycle while closing the current fuel cycle," in *European Nuclear Conference*, Brussels, 2007.
- [4] The Weinberg Foundation, "Thorium-Fuelled Molten Salt Reactors," June 2013. [Online]. Available: <http://www.the-weinberg-foundation.org/wp-content/uploads/2013/06/Thorium-Fuelled-Molten-Salt-Reactors-Weinberg-Foundation.pdf>. [Accessed 18 April 2014].
- [5] E. S. Bettis and R. C. Robertson, "The Design and Performance Features of a Single-Fluid Molten-Salt Breeder Reactor," *Nuclear Application and Technology*, vol. 8, pp. 190-207, 1970.
- [6] R. Cumberland and M. Yim, "A Computational Meta-Analysis of UCl₃ Cyclic Voltammograms in LiCl-KCl Electrolyte," *Journal of the Electrochemical Society*, vol. 161, no. 4, pp. D147-D149, 2014.
- [7] R. Cumberland, "1D and 3D Simulation of Electrochemical Behavior of U/UCl₃ and Pu/PuCl₃ in Molten Salt Systems (Master's Thesis)," Korean Advanced Institute of Science and Technology, Daejeon, South Korea, 2013.
- [8] J. Zhang, "Electrochemistry of Actinides and Fission Products in Molten Salts--Data Review," *Journal of Nuclear Materials*, vol. 447, pp. 271-284, 2014.

This is accepted pre-print of the article published in Journal of Nuclear Materials Management.

- [9] L. R. Morss, N. M. Edelstein and J. Fuger, *The Chemistry of the Actinide and Transactinide Elements*, Vol. 4, Dordrecht, Netherlands: Springer, 2006, pp. 2134-2135.
- [10] C. F. Baes, "The Chemistry and Thermodynamics of Molten-Salt-Reactor Fluoride Solutions," in *Thermodynamics*, Vol. 1, Vienna, 1966.
- [11] M. Iizuka, T. Inoue, O. Shirai, T. Iwai and Y. Arai, "Application of Normal Pulse Voltammetry to On-line Monitoring of Actinide Concentrations in Molten Salt Electrolyte," *J. Nucl. Matter*, vol. 297, pp. 43-51, 2001.
- [12] L. Cassayre, J. Serp, P. Soucek, R. Malmbeck, J. Rebizant and J.-P. Glatz, "Electrochemistry of Thorium in LiCl-KCl Eutectic Melts," *Electrochimica Acta*, vol. 52, pp. 7432-7437, 2007.
- [13] D. E. Peterson, "The Th-U (Thorium-Uranium) System," *Bulletin of Alloy Phase Diagrams*, vol. 6, no. 5, pp. 443-445, 1985.
- [14] F. A. Rough and A. A. Bauer, "Constitution of Uranium and Thorium Alloys," Battelle Memorial Institute, Columbus, OH, 1958.
- [15] P. Masset, R. Konings, R. Malmbeck, J. Serp and J.-P. Glatz, "Thermochemical Properties of Lanthanides (Ln = La, Nd) and Actinides (An = U, Np, Pu, Am) in the Molten LiCl-KCl Eutectic," *Journal of Nuclear Materials*, vol. 344, pp. 173-179, 2005.
- [16] R. B. Keithley, M. L. Heien and R. M. Wightman, "Multivariate Concentration Determination using Principal Component Regression with Residual Analysis," *Trends in Analytical Chemistry*, vol. 28, no. 9, pp. 1127-1136, 2009.
- [17] R. Kramer, *Chemometric Techniques for Quantitative Analysis*, New York, NY: Marcel Dekker, Inc., 1998.
- [18] I. T. Jolliffe, *Principal Component Analysis*, New York, NY: Springer Science, 2004.
- [19] M. M. Tylka, N. A. Smith, J. L. Willit and M. A. Williamson, "Electroanalytical Measurements of Uranium and Plutonium in Molten LiCl-KCl Eutectic," in *International Pyroprocessing Research Conference*, Fontana, WI, 2012.
- [20] G. Mamantov and F. R. Clayton, "Electrochemical Studies of Uranium and Thorium in Molten LiF-NaF-KF at 500° C," *Journal of the Electrochemical Society*, vol. 121, no. 1, pp. 86-90, 1974.

This is accepted pre-print of the article published in *Journal of Nuclear Materials Management*.

Citation details: Rappleye, D., Stika, M., & Simpson, M. F. (2014). Simulated Response of Electrochemical Sensors for Monitoring Molten-Salt Fueled Reactors. *Journal of the Institute of Nuclear Materials Management*, 43(1), 50–56.